Reversible and irreversible root phenotypic plasticity under fluctuating soil physical conditions

Sjulgård, Hanna; Iseskog, Daniel; Kirchgessner, Norbert; Bengough, Glyn; Keller, Thomas; Colombi, Tino

Published in:
Environmental and Experimental Botany

DOI:
10.1016/j.envexpbot.2021.104494

Publication date:
2021

Document Version
Publisher's PDF, also known as Version of record

Environmental and Experimental Botany 188 (2021) 104494

Contents lists available at ScienceDirect

Environmental and Experimental Botany

journal homepage: www.elsevier.com/locate/envexpbot

Reversible and irreversible root phenotypic plasticity under fluctuating soil physical conditions

Hanna Sjulgård [a], Daniel Iseskog [a], Norbert Kirchgessner [b], A. Glyn Bengough [c,d], Thomas Keller [a,e], Tino Colombi [a,*]

[a] Department of Soil and Environment, Swedish University of Agricultural Sciences (SLU), Box 7014, SE-75007, Uppsala, Sweden
[b] Institute of Agricultural Sciences, ETH Zurich, Universitätstrasse 2, CH-8092, Zurich, Switzerland
[c] The James Hutton Institute, Invergowrie, Dundee, DD2 5DA, UK
[d] School of Science and Engineering, University of Dundee, Dundee, DD1 4HN, UK
[e] Department of Agroecology and Environment, Agroscope, Reckenholzstrasse 191, CH-8046, Zürich, Switzerland

ARTICLE INFO

Keywords:
Phenotypic plasticity
Root growth
Root phenomics
Soil heterogeneity
Soil hypoxia
Soil penetration resistance

ABSTRACT

Roots grow in a highly heterogeneous physical environment due to the spatial complexity of soil structure. Thereby, the root growth zone repeatedly experiences soil physical stress such as hypoxia or increased penetration resistance. To mimic the highly variable physical environment surrounding the root growth zone, we subjected pea and wheat seedlings to periodic soil physical stress. One day of soil hypoxia or increased penetration resistance reduced root elongation rate of both species by at least 20 %. Upon stress release, root elongation rate of pea could recover within one day, while no such recovery occurred in wheat. Similarly, the diameter of the root elongation zone in pea increased by 15 % and 20 % due to hypoxia and increased penetration resistance, respectively, but decreased again once the stresses were released. In contrast, the diameter of the elongation zone of wheat roots started to decrease with the onset of soil physical stress and this trend continued upon stress release. Hence, root responses to short-term soil physical stress were reversible in pea and irreversible in wheat, indicating reversible and irreversible root phenotypic plasticity, respectively. This suggests that strategies to cope with periodic soil physical stress may vary among species. The differentiation between reversible and irreversible phenotypic plasticity is crucial to advance our understanding on soil exploration, resource acquisition, whole plant growth, and ultimately crop yield formation on structured soil.

1. Introduction

The spatial complexity of soil structure causes large heterogeneity in soil physical properties and conditions at the sub-millimetre scale (Dexter, 1988; Jin et al., 2013; Schlüter et al., 2019; Walter et al., 2009; Wang et al., 2020). Soil structure refers to the arrangement of solids and pores (Angers and Caron, 1998) and strongly influences soil physical properties that are key to root growth such as penetration resistance and soil oxygen concentration (Bengough et al., 2011; Jin et al., 2013). Low soil porosity and poor pore connectivity increase soil penetration resistance and impede gas transport in soil, which may decrease oxygen concentration in soil air and thereby lead to hypoxic conditions (Rabot et al., 2018). Moreover, soil moisture affects soil penetration resistance and soil oxygen concentration, which further contributes to the spatial heterogeneity of soil physical properties. Soil gas transport rates decrease with increasing soil moisture, while soil penetration resistance increases when soil dries (Bailey-Serres et al., 2012; Bengough et al., 2011; Whitmore and Whalley, 2009). Hence, roots inhabit a highly heterogeneous environment in which the mechanical stress at the root tip and the oxygen exchange rates between soil and roots change within millimetres. The root growth zone is therefore repeatedly exposed to soil physical stress as roots grow through soil. Understanding how plants respond to these heterogeneities and how this affects soil exploration and resource acquisition is crucial to improve the sustainability of crop production (Wang et al., 2020).

Soil physical stress such as soil hypoxia or increased soil penetration resistance directly affects root elongation rate and the metabolic costs of soil exploration (Bengough et al., 2011; Fukao and Bailey-Serres, 2004; Rich and Watt, 2013). Soil hypoxia typically occurs in response to flooding and soil compaction, and in naturally dense subsoil, and high

* Corresponding author:
E-mail address: tino.colombi@slu.se (T. Colombi).

https://doi.org/10.1016/j.envexpbot.2021.104494
Received 25 February 2021; Received in revised form 11 April 2021; Accepted 20 April 2021
Available online 25 April 2021

penetration resistance is characteristic for dry soil, compacted soil, and dense subsoil (Bengough et al., 2011; Fukao and Bailey-Serres, 2004; Lynch and Wojciechowski, 2015; Vaz et al., 2011; Weisskopf et al., 2010; Whitmore and Whalley, 2009). Cellular oxygen concentration decreases upon soil hypoxia, while the pressure roots must exert to grow through soil increases with greater penetration resistance. Low cellular oxygen concentration and increased pressure at the root tip reduce root elongation rate and thereby limit the access of plants to water and nutrients, which decreases crop productivity (Bengough et al., 2011; Fukao and Bailey-Serres, 2004; Jin et al., 2013; Saglio et al., 1984). Furthermore, soil hypoxia and high penetration resistance increase the metabolic costs of root growth. As a result, less carbon is available for aboveground plant growth and crop yield formation (Atwell, 1990a; Bailey-Serres et al., 2012; Colombi et al., 2019; Saglio et al., 1984). Yield reductions due to soil physical stress are already a prevalent problem (Bailey-Serres et al., 2012; Graves et al., 2015; Keller et al., 2019) and are likely to aggravate in the future. Dry and wet spells will become more frequent and severe due to climate change, while agricultural intensification involving heavy machinery will increase the area of compacted arable land (IPCC, 2014; Schjønning et al., 2015).

Plants can adjust their root phenotype to cope with soil physical stress. Axial and radial mechanical stress on the root tip as well as soil hypoxia often induce root thickening, which is mainly caused by an enlargement of the root cortex (Atwell, 1990b; Feng et al., 2020; Lipiec et al., 2012; Striker et al., 2007). Greater root diameter is related to higher root porosity and improved root aeration, which increases root growth under soil hypoxia (Broughton et al., 2015; Pedersen et al., 2020; Striker et al., 2007; Thomson et al., 1992). Root thickening also reduces the risk of root buckling and the mechanical stress at the root tip, which facilitates root growth under increased soil penetration resistance (Chimungu et al., 2015; Kirby and Bengough, 2002; Materechera et al., 1992). However, the metabolic costs of soil exploration increase with root thickening due to lower surface to volume ratio (Atwell, 1990a; Colombi et al., 2019; Eissenstat, 1992). Another way for plants to cope with soil physical stress is to increase root growth in spots with more favourable conditions. Plants may use macropores as pathways of least resistance or as a source of oxygen (Athmann et al., 2013; Atkinson et al., 2020; Colombi et al., 2017a; White and Kirkegaard, 2010). Similarly, root growth in zones with higher porosity can be prioritized over growth in zones with low porosity (Bingham and Bengough, 2003; Pfeifer et al., 2014). However, due to soil structural heterogeneity, spots of favourable soil physical conditions are spatially limited and roots will eventually re-enter zones in which they are exposed to soil physical stress.

Root phenotypic plasticity, i.e. the ability to adjust the root phenotype to changing edaphic conditions, is crucial for whole plant growth (Correa et al., 2019; Lobet et al., 2018; Schneider and Lynch, 2020; Ye et al., 2018). As roots grow through soil, the physical conditions around the root growth zone are constantly changing. Thus, phenotypic plasticity includes adjustments of the root phenotype to soil physical stress as well as adjustments in response to the release of soil physical stress. It has been shown that phenotypic responses of pea roots such as root elongation rate and root diameter to soil physical stress are reversible upon stress release (Bengough and Mackenzie, 1994; Croser et al., 2000, 1999; Malik et al., 2015), while in cereals these responses persist upon stress release (Malik et al., 2002; Watkin et al., 1998). This suggests that root phenotypic responses to fluctuating soil physical conditions can be reversible or irreversible. Since roots grow in a physically heterogeneous environment, distinguishing between irreversible and reversible phenotypic plasticity is critical to advance our knowledge on root growth and plant development on structured soil. In previous studies investigating root responses to fluctuating soil physical conditions, penetration resistance and soil oxygen concentration were changed after several days to weeks (Croser et al., 2000, 1999; Malik et al., 2015, 2002; Watkin et al., 1998). However, the physical environment surrounding the root growth zone fluctuates much faster since soil physical conditions change within millimetres (Dexter, 1988; Jin et al., 2013; Walter et al., 2009; Wang et al., 2020). Hence, experiments in which soil physical stress is applied for short periods are needed to better understand how roots grow in structurally heterogeneous soil.

In the current study, we grew pea (*Pisum sativum*, L.) and wheat (*Triticum aestivum*, L.) seedlings under fluctuating soil physical conditions. To mimic the variability of the physical environment surrounding the root growth zone, soil penetration resistance or the oxygen concentration of the soil atmosphere were changed in one-day intervals. We hypothesized that phenotypic strategies to cope with the periodic occurrence of short-term soil physical stress differ between pea and wheat. Time-lapse imaging was deployed to record root elongation rate and the temporal development of root diameter and root anatomical traits were quantified.

2. Material and methods

2.1. Rhizobox design

We designed rhizoboxes that allowed for independent controlling of the oxygen concentration of the air in the growth substrate and the substrate density and thus substrate penetration resistance. The rhizoboxes were manufactured from Polylactide (PLA) plastic using a benchtop 3D printer (Ultimaker 3 Extended, Ultimaker, Utrecht, Netherlands). The growth compartment of the rhizoboxes was located at the front side of the rhizoboxes and was 120 mm high, 40 mm wide and 14 mm deep. This compartment was filled with growth substrate (described below), and roots grew into it through a hole in the top of the compartment. The front side of the growth compartment was tightly closed with a transparent Plexiglass cover (Fig. 1A).

Air channels, which were open towards the growth substrate, ran vertically through the frame of the growth compartment (Fig. 1A). Hypoxia was induced by flushing nitrogen gas (N_2) through these channels for one minute before connecting the growth compartments to a 25 L gas-sampling bag (Altef Gas Sammpling Bag, Teknolab Sorbent, Kungsbacka, Sweden) that was filled with N_2. To release hypoxia, the growth compartments were disconnected from the gas sampling bag and flushed with ambient air for one minute. A pressure block of 112 mm height and 32 mm width was located at the back side of the growth compartment. This block was fixed with a one-millimetre thick elastic rubber sheet to a rigid frame. A bicycle tube (length/width: 120/40 mm) was positioned behind the pressure block. The tube was kept in place by a case that was attached to the frame holding the pressure block. By inflating the tube, the pressure block moved towards the growth compartment, thereby compressing the growth substrate (Fig. 1A). Due to the tension of the rubber sheet with which the pressure block was attached to the frame, the pressure on the substrate could be reversed by releasing the air from the bicycle tube.

2.2. Soil physical conditions

Plants were grown in commercial potting substrate (Reko-jord, Hasselfors garden, Hasselfors, Sweden) that was sieved at 4 mm. The substrate had an organic matter content of 41 %, the mineral fraction consisted of 22 % clay, 41 % silt and 37 % sand, and the average particle density of the substrate was 2.07 g cm^{-3}. Substrate was evenly packed to a bulk density of 0.36 g cm^{-3} through the open front side of the growth compartment and the growth compartment was closed with the Plexiglas cover. The volumetric water content of the growth substrate was 0.45 m m^{-3}, corresponding to −25 kPa matric potential. The oxygen concentration of the air in the growth substrate was measured with a portable gas analyser (CheckPoint 3, Dansensor, Ringsted, Denmark). Flushing the growth compartment with N_2 immediately decreased the oxygen concentration from 21 % (ambient conditions) to 3 % (hypoxia; Table 1).

Inflating the bicycle tube to 100 kPa increased substrate bulk density

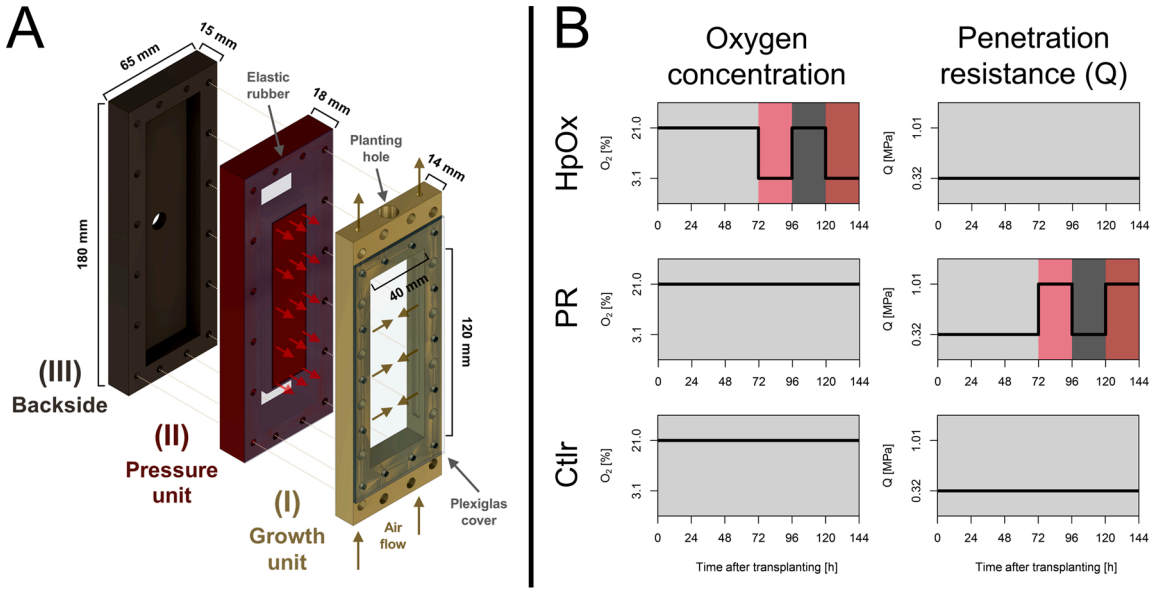

Fig. 1. (A) Illustration of rhizoboxes consisting of three separate units: (I) Growth compartment that was filled with growth substrate and covered with a transparent Plexiglas cover. Roots grew into the compartment through a hole at the top of the compartment. Oxygen concentration of the air within the substrate was controlled through air channels in the frame of the compartment (beige arrows); (II) Pressure block fixed with an elastic rubber sheet to a frame. Inflating the bicycle tube placed behind the pressure block increased substrate bulk density (red arrows) and thus substrate penetration resistance; (III) Rigid backside used to keep bicycle tube in place. (B) Schematic representation of soil physical conditions roots were exposed to under periodic occurrence of hypoxia (HpOx), under periodically increased penetration resistance (PR) and under optimal growth conditions (Ctrl). (For interpretation of the references to colour in the Figure, the reader is referred to the web version of this article).

Table 1
Particle density (ρ_p), bulk density (ρ_b), total porosity (ε), volumetric water content (θ), air-filled porosity (ε_a), oxygen concentration in substrate air (O_2), and substrate penetration resistance (Q) under optimal growth conditions and periodic soil physical stress.

	Treatment		
Soil physical property	Ctrl	HpOx	PR
ρ_p [g cm^{-3}]		2.07	
ρ_b [g cm^{-3}]	0.36	0.36	0.46
ε [m^3 m^{-3}]	0.83	0.83	0.78
θ [m^3 m^{-3}]	0.46	0.46	0.58
ε_a [m^3 m^{-3}]	0.37	0.37	0.20
O_2 [%]	21.0	3.1	21.0
Q [MPa]	0.32	0.32	1.01

Abbreviations: Ctrl = optimal growth conditions; HpOx = periodic hypoxia; PR = periodically increased penetration resistance; SE = standard error.

by 28 %. This deformation of the substrate was reversed within minutes after releasing the pressure from the tube (Supplemental Fig. S1). Substrate penetration resistance was measured in soil cylinders (height/diameter: 50/72 mm) that were packed to bulk densities reflecting loose and compressed growth substrate. Penetration force was recorded with two 50 N load cells (S2M/50 N, HBM GmbH, Darmstadt, Germany) that were connected via an aluminium plate to a cone penetrometer. The cone had a recessed shaft, a base diameter of 5 mm, and an opening angle of 60°. It was inserted 25 mm into the substrate at a penetration speed of 12 mm min^{-1}. Data were considered from the point the cone was fully inserted into the substrate, and penetration resistance was obtained by dividing the recorded force by the cone base area. Compressing the substrate increased penetration resistance from 0.32 MPa to 1.01 MPa (Table 1). Before starting the experiments, the substrate was compressed and then decompressed to ensure the same starting conditions across treatments.

2.3. Plant material and experimental set-up

Experiments were conducted with pea (variety: Ingrid) and wheat (variety: Rohan). Pre-germinated seeds (72 h, 19.2 °C) with radicles of similar lengths (~3 mm) were selected and transplanted into small substrate-filled plastic funnels. The funnels were firmly inserted into the hole located at the top of the growth compartment (Fig. 1A). To minimize evaporation, the funnels were covered with aluminium foil. Emerging leaves could grow through a small hole in the foil. We attached the rhizoboxes to an aluminium frame at an inclination angle of 30° with the Plexiglas cover facing downwards. The frame had space for twelve rhizoboxes and was placed into a growth chamber set to 12 h day length, an average temperature of 19.2 °C, and a relative humidity of 58 %. To avoid that roots were exposed to visible light, we covered the frame with black rubber sheets.

For the first three days, plants were grown under optimal conditions. During the fourth day after transplanting, we exposed roots to either hypoxia or increased substrate penetration resistance. Stress was released after one day, and plants were grown under optimal conditions during the fifth day after transplanting. Finally, roots were exposed again to hypoxia or increased penetration resistance during the sixth day after transplanting. A control treatment with optimal growth conditions for six days complemented the treatments. Hence, the soil physical conditions were the same in the control treatment and in two the treatments with periodic soil physical stress during the first three days of the experiments (Fig. 1B). All treatment-species combinations were replicated four times (n = 4).

2.4. Time-lapse imaging

Time-lapse imaging with a 24-megapixel camera (Canon EOS 750d, Canon, Tokyo, Japan) that had the infrared filter removed was used to record root elongation under infrared illumination. Two rows of 20 LEDs with a wavelength of 830 nm (TSHG8400 Vishay, 830Nm IR LED, Vishay Intertechnology, Inc., Malvern, PA, USA) were placed vertically at both sides of the camera lens. The camera was equipped with a macro

lens (EF-S 35 mm f/2.8 Macro IS STM, Canon, Tokyo, Japan) and was set to an exposure time of 1/3 s, a film speed of 100 ISO, and an aperture value of f/13.

The camera and the illumination system were fixed to a camera dolly, which was attached to an aluminium rail (Norcan, Haguenau Cedex, France). A stepper motor (Nema 17 Bipolar 1.8deg 45Ncm, Fulling Motor Co., Ltd., Changzhou, China) that was connected to the dolly via a gearwheel and a rubber timing belt controlled the movement of the dolly. The motor was operated with an Arduino microcontroller (Arduino Mega 2560, Arduino AG, Somerville, MA, United States) and a motor driver (Adafruit Motor Shield V2, Adafruit Industries, New York City, NY, United States). The same microcontroller was used to trigger the camera shutter. To ensure constant time-intervals (20 min) between pictures from the same rhizobox, a timer was implemented using a second microcontroller (Arduino Micro).

2.5. Quantification of root elongation rate

Four round black position markers were attached to the Plexiglass at a horizontal distance of 42.5 mm. The central coordinates of these markers were determined automatically for each picture using ImageJ (version 1.51 r; National Institute of Health, Bethesda, MD, United States) to quantify the pixel edge length (19.5 µm) and to correct for horizontal drift in the camera position caused by slight inconsistencies of the stepper motor.

We quantified root elongation rates of all visible axial roots, i.e. the primary root in pea and primary and seminal roots in wheat. Root tips became visible during the third day after transplanting and root elongation rate could therefore be assessed during the fourth, fifth and sixth day after transplanting. The coordinates of root tips were manually determined in every picture taken during this period. Image acquisition times were extracted from original images using R version 3.4.1 (R Core Team, 2017) and the 'exiftoolr' package (O'Brien, 2019), and merged with root tip coordinate data. The elongation rate of individual roots ($E_r(t)$) in mm h^{-1} was then calculated as:

$$E_r(t) = \frac{1}{\Delta t}\sqrt{\left[(x_{t-1} - x_t)^2 + (y_{t-1} - y_t)^2\right]} \quad (1)$$

where x and y denote root tip coordinates at time point t and t-1. Occasionally, root tips were growing away from the Plexiglas and were therefore not visible in the pictures, resulting in gaps in root tip coordinate measurements. In these cases, root elongation rates were linearly interpolated based on root tip coordinates before and after the gap occurred. Root length was obtained by integrating root elongation rates over time. We assessed the accuracy of this approach by comparing calculated root length with root length measurements that were determined manually from pictures taken after four, five and six days of growth. Since the number of visible roots in wheat varied between one and four roots, average elongation rate and length of all visible roots were calculated.

2.6. Root diameter and root anatomy measurements

Six days after transplanting, roots were washed out from the growth substrate. The roots that were visible at the Plexiglas cover were preserved in 70 % [v/v] ethanol and stored at 4 °C until further processing. Roots were scanned in a flatbed scanner at 1200 dpi (Epson Perfection V800, Seiko Epson Corporation, Suwa, Nuagano, Japan; pixel edge length: 21.2 µm). From these scans, root diameters were determined manually at 72 positions along the root axis, representing the development of the diameter of the root elongation zone at hourly intervals. As suggested by Yamauchi et al. (2020), these positions were determined based on root elongation rates (Eq 1). Diameters were measured 10 mm (pea) and 5 mm (wheat) behind the position where the root tip was located at the respective time step.

Bright field microscopy (Kern Optics OBF 122; Kern & Sohn GmbH, Balingen, Germany) was used to quantify root anatomical traits. Roots were divided into three segments, corresponding to the fourth, the fifth and the sixth day after transplanting. Cross sections of approximately 150 µm thickness were taken manually with a razorblade from the middle of each segment, and stained with Toluidine Blue (0.1 % [w/v] in distilled water). Images of these cross sections were acquired at 100x magnification with a microscope camera (Mirazoom MZ808; Oowl Tech Limited, Hong Kong, China; pixel edge length: 0.7 µm). Total cross section area and stele area were measured manually from these pictures and root cortex area was obtained by subtracting stele area from total cross section area. The number of root cortical cell files excluding epi- and endodermal cells was determined. Mean root cortical cell size was quantified by measuring the cross sectional area of 15 cortical cells across cortical cell files.

2.7. Statistical analysis

Data analysis was carried out in R. Linear mixed models were used to evaluate effects of soil physical stress, the day after transplanting, and their interaction on daily mean root elongation rate, daily mean root diameter, and root anatomical traits. The following model was applied separately to both species using the 'nlme' package (Pinheiro et al., 2013):

$$Y_{ijk} = \alpha_i + \beta_{ij} + \alpha\beta_{ij} + \gamma_k + r_{ijk} \quad (2)$$

where Y denotes the tested root trait of the ith treatment (i = optimal conditions, hypoxia, increased penetration resistance), the jth day after transplanting ($j = 4, 5, 6$), and the kth sample (k = 1, 2, 3, …, 12). Effects of the treatment (α), the time after transplanting (β), and their interaction ($\alpha\beta$) were set as fixed factors. The sample effect (γ) was added as a random factor to account for repeated measurements. The residual error is denoted by r. Fixed effects were tested for significance using analysis of variance. Treatment means within the same day after transplanting were compared using analysis of variance and least significant difference (LSD) tests as implemented in the 'agricolae' package (de Mendiburu, 2017). Linear regression models were applied to compare calculated and manually measured root lengths and to relate different root anatomical traits. Non-linear regression models were applied to assess the temporal development of the root elongation zone diameter.

3. Results

3.1. Responses of root elongation rate to periodic soil physical stress

Calculated and manually measured root length were strongly correlated ($R^2 = 0.996$, slope = 1.025 ± 0.008 (standard error), $p < 0.001$; Supplemental Fig. S2). Thus, root elongation rate and root length could be accurately quantified using root tip coordinates. Daily root elongation rate of pea and wheat grown under optimal soil physical conditions during the entire experiment did not change significantly over time (Supplemental Fig. S3). Soil physical stress significantly affected daily root elongation rate of pea ($p < 0.01$) and wheat ($p < 0.001$). Significant effects of the time after transplanting on root elongation rate occurred in pea ($p < 0.001$) but not in wheat ($p = 0.07$; Table 2).

In pea, root elongation rate decreased significantly in response to the first exposure to soil physical stress. Root elongation rate was more than 25 % lower under hypoxia ($p < 0.01$) or increased penetration resistance ($p < 0.05$) than under optimal growth conditions. Releasing soil physical stress resulted in a recovery of root elongation rate in pea. No significant differences in root elongation rate between previously stressed plants and plants grown under optimal conditions occurred upon stress release.

Table 2
Effects of treatment (Trt), time after transplanting (Time), and their interaction (Trt:Time) on daily mean root elongation rate, daily mean diameter of the root elongation zone, root cross section area, and root cortical area evaluated with linear mixed models (Eq 2) followed by analysis of variance. ***, **, and * denote significant effects at $p < 0.001$, 0.01 and 0.05 ($n = 4$).

Trait	Species	Trt	Time	Trt:Time
E_r [mm h^{-1}]	Pea	**	***	0.13
	Wheat	***	0.07	0.17
Rdm [mm]	Pea	0.15	***	*
	Wheat	**	***	***
RCsA [mm^2]	Pea	0.06	***	*
	Wheat	**	***	*
CorA [mm^2]	Pea	0.06	***	*
	Wheat	**	***	**

Abbreviations: E_r= root elongation rate; Rdm = root diameter, RCsA = root cross section area; CorA = root cortex area.

In response to the second exposure to soil physical stress, root elongation rate of pea decreased again. Root elongation rate was 25%–40% lower under the second period of soil physical stress than under optimal growth conditions ($p < 0.01$; Fig. 2). Daily root elongation rate of wheat also significantly decreased in response to the first exposure to hypoxia or increased penetration resistance ($p < 0.01$). In contrast to pea, root elongation rate of wheat did not recover upon stress release. Previously stressed plants showed 20 % lower root elongation rate than plants grown under optimal conditions ($p < 0.01$). During the second period of soil physical stress, wheat root elongation rate was more than 30 % lower under hypoxia or increased penetration resistance than under optimal growth conditions (Fig. 2).

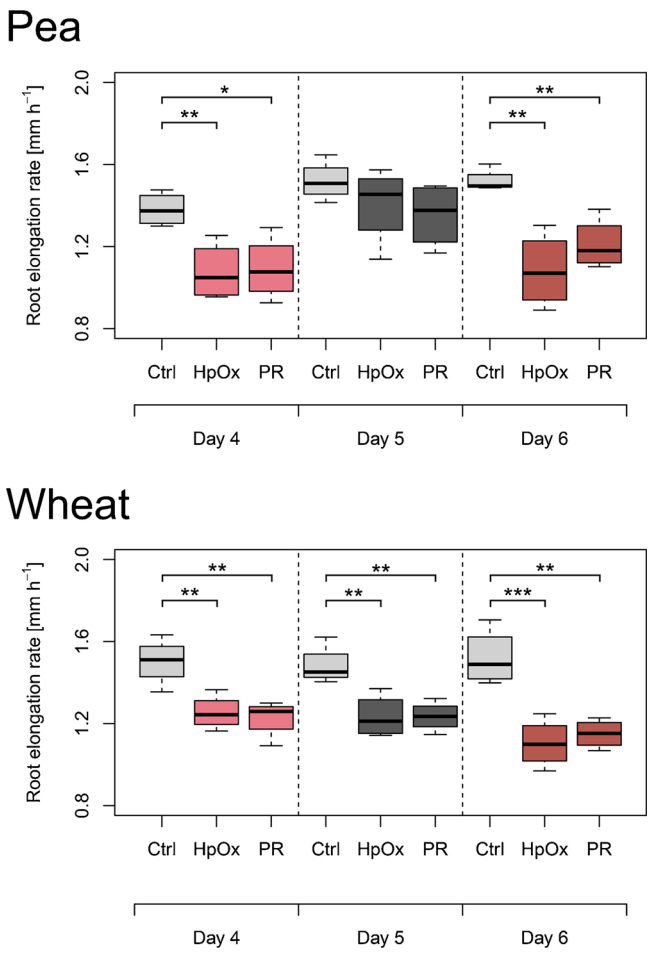

Fig. 2. Daily root elongation rate of (top) pea and (bottom) wheat under fluctuating soil physical conditions. Roots were exposed to hypoxia (HpOx) or increased penetration resistance (PR) during day four (light red) and day six (dark red), and subjected to optimal growth conditions during day five (dark grey), or grown under continuous optimal conditions (Ctrl, light grey). ***, ** and * denote significant differences between treatment means based on least significant difference tests at $p < 0.001$, 0.01 and 0.05, respectively ($n = 4$). (For interpretation of the references to colour in the Figure, the reader is referred to the web version of this article).

The different responses to stress release between pea and wheat were further highlighted by plotting the difference in root length over time between plants grown under optimal soil physical conditions and plants that were periodically exposed to hypoxia or increased penetration resistance. In wheat, the difference in root length between plants grown under optimal conditions and plants grown under fluctuating soil physical conditions increased at a similar rate during the entire experiment. In pea, however, this rate was clearly lower during the period of stress release than during stress exposure, indicating the recovery of root elongation rate upon the release of soil physical stress (Fig. 3).

3.2. Temporal development of root diameter under periodic soil physical stress

Significant effects of the time after transplanting ($p < 0.001$) on daily mean diameter of the root elongation zone occurred in both species (Table 2). Significant temporal changes were observed under fluctuating soil physical conditions but not under optimal growth conditions (Supplemental Fig. S4). Similar to root elongation rate, the temporal development of the diameter of the root elongation zone under fluctuating soil physical conditions differed between pea and wheat (Fig. 4).

Pea roots started to thicken with the onset of the first period of soil physical stress. The diameter of the root elongation zone in pea increased by 15 % during the first eight hours of hypoxia, and by 20 % during the first twelve hours of increased penetration resistance. After this initial increase, the diameter of the elongation zone decreased until the end of the first period of soil physical stress and this trend continued upon stress release. One day after soil physical stress was released, the diameter of the elongation zone was comparable between previously stressed plants and plants grown under optimal conditions. Remarkably, no thickening of the root elongation zone occurred in response to the second exposure to soil physical stress (Fig. 4). In wheat, the diameter of the root elongation zone decreased already by 10 % during the first period of hypoxia or increased penetration resistance. Although this trend slowed down, it continued upon stress release and during the second period of hypoxia or increased penetration resistance. At the end of the second period of soil physical stress, the diameter of the root elongation zone was 20 % lower under fluctuating soil physical conditions than under constant optimal conditions (Fig. 4).

In both species, the temporal development of the diameter of the root elongation zone under fluctuating soil physical conditions could be explained with non-linear regression models. In pea, quartic polynomial regressions explained 84 % and 89 % of the variation under periodic exposure to hypoxia or increased penetration resistance, respectively. Under fluctuating soil physical conditions, the temporal development of the diameter of the root elongation zone in wheat followed exponential decay models, yielding R^2 values greater than 0.85 (Fig. 4). Significant regression coefficients were obtained for polynomial (Supplemental Table S1) and exponential models (Supplemental Table S2).

3.3. Root anatomical traits underlying changes in root diameter

The effects of periodic soil physical stress on root cross section area, which represents a surrogate measurement for root diameter, coincided with the effects of soil physical stress on daily mean root diameter (Table 2). In both species, the temporal development of root cross section area (Supplemental Fig. S5) was comparable to the development of daily mean diameter of the root elongation zone (Supplemental Fig. S4).

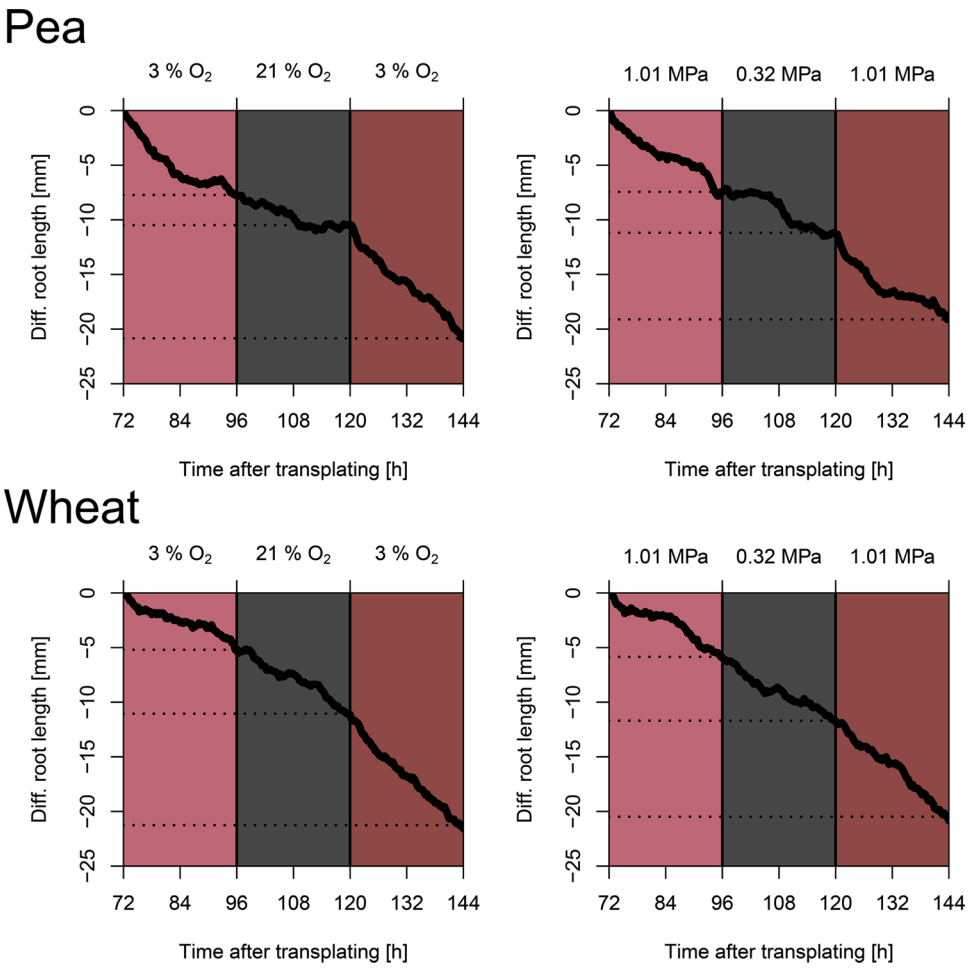

Fig. 3. Difference in root length between plants grown under optimal growth conditions and plants periodically exposed to soil physical stress in (top) pea and (bottom) wheat. Light and dark red background represent period of soil physical stress and dark grey background represents period of released stress, i.e. optimal growth conditions. Dashed lines denote difference in root length at the end of the first and second period of soil physical stress and at the end of the period of released stress. Plotted values represent average of four replicates (n = 4). (For interpretation of the references to colour in the Figure, the reader is referred to the web version of this article).

The changes of root cross section area and thus root diameter due to soil physical stress were mainly related to alterations of the root cortex area (Fig. 5). Cortex area showed significant responses to the day after transplanting in pea and wheat ($p < 0.001$; Table 2) and changed significantly over time under fluctuating soil physical conditions but not under optimal growth conditions (Supplemental Fig. S6). In both species, less pronounced responses to fluctuating soil physical conditions occurred for stele area (Supplemental Table S3 and S4) and cortex area was the stronger predictor for cross section area than stele area (Supplemental Fig. S7).

Root cortex area in pea increased in response to the first exposure to soil physical stress, particularly under increased penetration resistance. After this initial increase, root cortex area decreased again and was comparable between plants exposed to fluctuating soil physical conditions and plants grown under optimal conditions (Table 3). In wheat, the periodical exposure to hypoxia or increased penetration resistance resulted in decreased root cortex area. Significant differences ($p < 0.01$) in root cortex area between plants grown under optimal conditions and plants exposed to fluctuating soil physical conditions occurred during the period of released stress and the second period of soil physical stress (Table 3). In pea, changes in cortical area were mostly associated with changes in cortical cell size, while changes in cortical area of wheat roots coincided with changes in cortical cell size and cortical cell file number (Supplemental Table S3 and S4).

4. Discussion

4.1. Mimicking soil heterogeneity through short-term fluctuations of soil physical conditions

To mimic the variable physical environment that roots encounter as they grow through soil (Dexter, 1988; Jin et al., 2013; Walter et al., 2009; Wang et al., 2020), we designed rhizoboxes that allowed changing soil physical conditions at short time intervals (Fig. 1). Water logging and drainage results in rather slow changes of the oxygen concentration of soil air (Araki et al., 2012; Malik et al., 2015, 2002) and affects soil moisture and thus soil penetration resistance (Bengough et al., 2011; Vaz et al., 2011; Whitmore and Whalley, 2009). Directly altering the gas composition of the soil atmosphere as done here and elsewhere (Gill and Miller, 1956), resulted in rapid changes of soil oxygen concentration without affecting soil moisture or soil mechanical properties (Table 1). Similar to previous studies (Barley, 1962; Gill and Miller, 1956; Goss, 1977; Young et al., 1997), soil penetration resistance was increased by compressing the growth substrate. In our set-up, the growth substrate was compressed from the back (Fig. 1A), which most likely resulted in a combination of axial and radial mechanical stress. Due to the elasticity of the growth substrate used in the current study (Supplemental Fig. S1), penetration resistance could be decreased again by releasing the pressure from the growth substrate (Table 1). Thus, plants could be grown in a dynamically changing yet controlled soil physical environment, and oxygen concentration and penetration resistance could be varied independently during experiments.

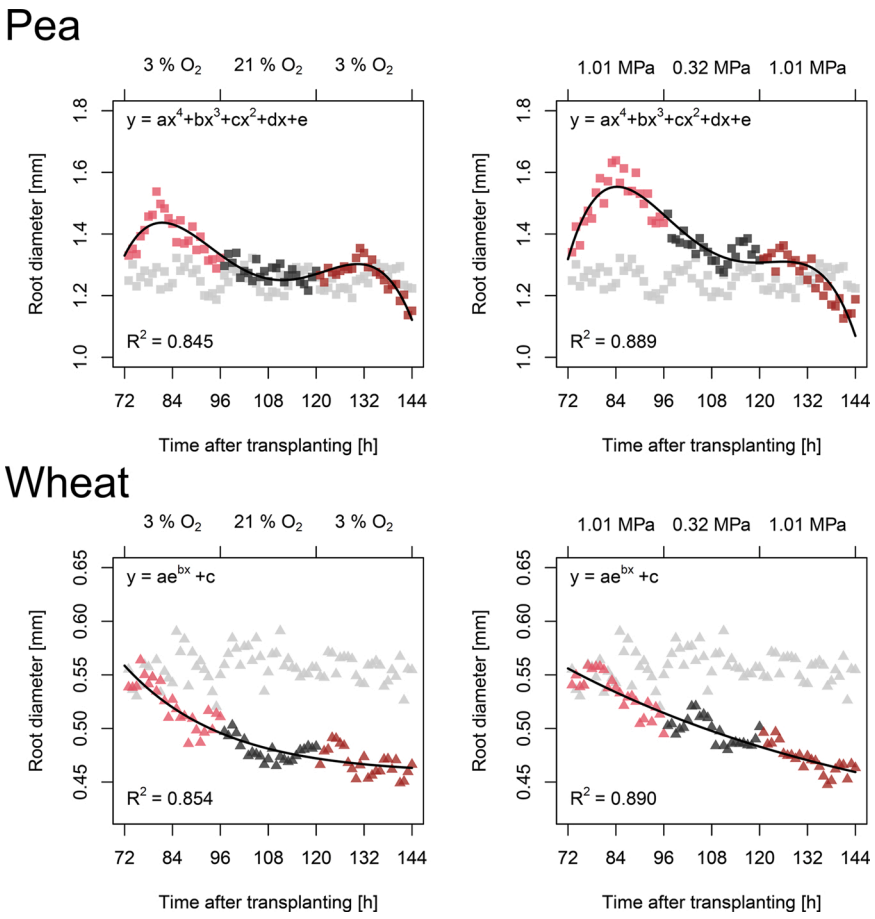

Fig. 4. Temporal development of the diameter of the root elongation zone in (top) pea and (bottom) wheat under fluctuating soil physical conditions. Light and dark red symbols represent periods of soil physical stress and dark grey symbols represent period of released stress, i.e. optimal growth conditions. Light grey symbols represent diameter of the root elongation zone in plants that were constantly exposed to optimal growth conditions. R^2 represents multiple r-squared and plotted values represent average of four replicates (n = 4). Regression coefficients are provided in Supplemental Tables S1 and S2. (For interpretation of the references to colour in the Figure, the reader is referred to the web version of this article).

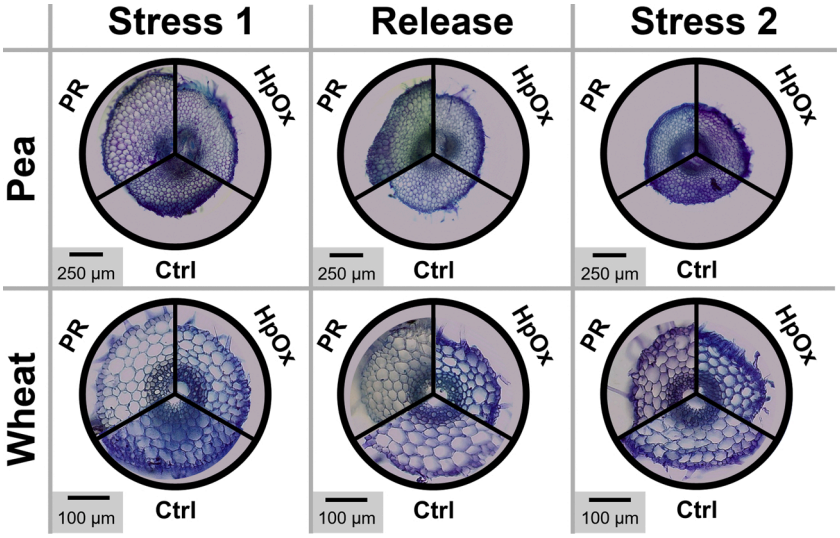

Fig. 5. Typical pictures of (top) pea and bottom (wheat) root cross sections depicting root anatomy during periods of soil physical stress (Stress 1, Stress2) and period of released stress, i.e. optimal growth conditions (Release). Roots of stressed plants were subjected to periodically occurring hypoxia (HpOx) and periodically increased penetration resistance (PR). Ctrl represents roots of plants that were that were constantly exposed to optimal growth conditions.

4.2. Pea and wheat responded differently to short-term fluctuations of soil physical conditions

Short-term exposure to soil hypoxia or increased penetration resistance caused alterations of the root phenotype of pea and wheat. Previous studies reported that several days of soil physical stress slow down root elongation in pea and wheat (Araki et al., 2012; Croser et al., 2000, 1999; Malik et al., 2015, 2002; Watkin et al., 1998). Furthermore, it has been shown that root elongation rate of pea and other grain legumes such as lentils recovers within several days to weeks after the stress is released (Croser et al., 2000, 1999; Malik et al., 2015), while no such recovery was observed in wheat (Malik et al., 2002; Watkin et al., 1998).

Table 3
Treatment effects (Trt) on root cortex area during the first exposure to soil physical stress (Stress 1), the period of stress release (Release), and the second exposure to soil physical stress (Stress 2) evaluated with analysis of variance. ** and * denote significant effects at $p < 0.01$ and < 0.05, respectively. Values represent treatment means and LSD denotes least significant difference at $p < 0.05$ ($n = 4$).

			Root cortex area [mm^2]			
Species	Period	Trt	Ctrl	HpOx	PR	LSD
Pea	Stress 1	*	0.665	0.733	0.980	0.230
	Release	0.22	0.567	0.584	0.672	0.135
	Stress 2	0.26	0.586	0.542	0.526	0.079
Wheat	Stress 1	0.12	0.119	0.100	0.116	0.020
	Release	**	0.119	0.076	0.092	0.019
	Stress 2	**	0.112	0.072	0.082	0.017

Abbreviations: Ctrl = optimal growth conditions; HpOx = periodic hypoxia; PR = periodically increased penetration resistance.

Here we provide evidence that these patterns also occur when soil physical conditions change at much shorter time intervals. Exposing pea for one day to soil physical stress resulted in significantly reduced root elongation rate. Upon decreased penetration resistance, root elongation rate of pea recovered considerably within one day (Figs. 2 and 3), corroborating results from a previous study (Bengough and Mackenzie, 1994). Similarly, root elongation rate of pea recovered almost completely after the release of hypoxia (Figs. 2 and 3). In wheat, one day of hypoxia or increased penetration resistance also significantly decreased root elongation rate. Other than in pea, root elongation rate of wheat did not recover upon stress release. Roots of previously stressed plants elongated significantly slower than roots of plants that were never exposed to soil physical stress (Figs. 2 and 3). These results highlight that responses of root growth dynamics to fluctuations of the physical conditions around the root growth zone, which typically occur in soil (Dexter, 1988; Jin et al., 2013; Walter et al., 2009; Wang et al., 2020), can differ significantly between species.

The temporal development of diameter of the root elongation zone under fluctuating soil physical conditions also differed between pea and wheat. In both species, these diameter changes were mainly related to alterations of the root cortical area (Fig. 5, Supplemental Fig. S7), which corroborates previous findings (Atwell, 1990b; Lipiec et al., 2012; Striker et al., 2007). The elongation zone of pea roots started to thicken with the onset of the first period of soil hypoxia or increased penetration resistance. After this initial increase, however, pea roots became thinner again and no re-thickening occurred upon the second exposure to soil physical stress (Fig. 4). In wheat, the diameter of the elongation zone started to decrease already during the first period of soil hypoxia and increased penetration resistance. This trend continued at a slower rate upon stress release and during the second period of soil physical stress (Fig. 4). Root thickening in responses to axial (Bengough and Mackenzie, 1994; Chimungu et al., 2015; Kirby and Bengough, 2002; Materechera et al., 1992) and radial mechanical stress (Feng et al., 2020; Kolb et al., 2012) reduces the mechanical stress at the root tip and the risk of root buckling. Furthermore, thicker roots are associated with greater root porosity and improved root aeration under reduced soil oxygen concentration (Pedersen et al., 2020; Striker et al., 2007). Hence, root thickening may help plants to withstand soil physical stress. However, it has been highlighted that these responses strongly depend on the severity of the applied soil physical stresses (Iijima and Kato, 2007; Lipiec et al., 2012; Nosalewicz and Lipiec, 2014; Shierlaw and Alston, 1984; Tracy et al., 2013). Moreover, the metabolic costs of root growth increase with root diameter and these costs are particularly high under soil hypoxia and increased penetration resistance (Atwell, 1990a; Colombi et al., 2019; Eissenstat, 1992; Fukao and Bailey-Serres, 2004). Thus, there are trade-offs between the metabolic costs of root growth and the ability of plants to withstand soil physical stress. Our study indicates that regulating metabolic costs of root growth can affect responses in root diameter to fluctuating soil physical conditions.

4.3. Strategies to cope with periodic soil physical stress differed between species

Our study on single genotypes suggests that pea and wheat may have different strategies to cope with the periodical exposure to soil physical stress. In wheat, initial responses to soil physical stress such as reduced root elongation rate (Fig. 2), root thinning (Fig. 4), and decreased root cortex area (Fig. 5) persisted or became even more pronounced upon stress release and repeated stress exposure. In contrast, root phenotypic responses of pea to the first period of soil hypoxia or increased penetration resistance were not persistent. Root elongation rate recovered significantly upon stress release (Fig. 2) and the initial increase in root diameter (Fig. 4) and root cortical area (Fig. 5) was reversed once the stress was released. These different patterns suggest that the observed responses of pea roots to fluctuating soil physical conditions can be described as reversible phenotypic plasticity, while irreversible phenotypic plasticity characterized the responses of wheat roots.

As in other legumes, soil exploration in pea largely depends on the extension of the primary root, which forms the main axis of the entire root system. In plants with a fibrous root system such as wheat, new axial roots are initiated throughout the plant life cycle (Lynch, 2013). We propose that this fundamental difference in root system structure may explain the difference between pea and wheat regarding their strategy to cope with periodic soil physical stress. Reversible phenotypic plasticity of the primary root as observed here and elsewhere (Croser et al., 2000, 1999; Malik et al., 2002) enables pea to respond immediately to changes in the soil physical environment. Increasing root elongation under favourable soil physical conditions allows pea to reach deeper into the soil. Similarly, if the environment allows, pea can reduce the diameter of its primary root, which saves carbon that can be used for lateral root growth or aboveground plant development. In contrast, wheat may compensate the impeded extension of its seed-borne roots by increasing the growth rate of nodal roots, which has been observed in response to reaeration (Malik et al., 2002; Watkin et al., 1998). Root thinning can then reduce the metabolic cost needed for the growth of seed-borne roots. However, a greater investment into nodal root growth is also likely to increase the overall metabolic costs of soil exploration because nodal roots are thicker than seed-borne roots (Atwell, 1990a; Eissenstat, 1992; Lynch, 2013). Moreover, since seed-borne roots reach deeper into the soil than nodal roots (Araki and Iijima, 2001; Belford et al., 1987), prioritizing nodal root growth may reduce rooting depth and thus potential exploration of subsoil resources.

4.4. Differentiating between reversible and irreversible phenotypic plasticity to account for belowground heterogeneity

It has been highlighted that root phenotypic plasticity is crucial for plants to cope with edaphic abiotic stress (Correa et al., 2019; Lobet et al., 2018; Schneider and Lynch, 2020; Ye et al., 2018). Soil physical properties such as oxygen concentration of the soil atmosphere or penetration resistance show high spatial variability (Jin et al., 2013; Walter et al., 2009; Wang et al., 2020). Hence, a single root repeatedly encounters suboptimal and optimal conditions as it grows through soil. Here, we demonstrate that short-term periodic exposure to soil physical stress has profound effects on the root phenotype and that these effects may differ substantially between species. Phenotypic responses of pea roots were largely reversible, while in wheat these responses were irreversible, which indicates that the strategy to cope with fluctuating soil physical conditions differs between species. In our set-up, the entire root system was exposed to fluctuating soil physical conditions, while physical conditions in structured soil may differ between roots of the same plant as well as along a single root axis. Set-ups that allow controlling the physical environment around single roots and thereby exposing different root classes to soil physical stress could provide

further insights into plant responses to changing soil physical conditions.

Here we investigated responses to fluctuating soil physical conditions of one pea and one wheat genotype. However, genotypes of the same species can differ in their susceptibly to soil physical stress (Broughton et al., 2015; Chimungu et al., 2015; Colombi et al., 2017b), suggesting that strategies to cope with fluctuating soil physical conditions also differ among genotypes. Such genotypic differences can potentially be explored to develop novel crop cultivars that are better adapted to heterogeneous soil physical conditions. In the current study, we focused on the heterogeneity of soil physical conditions, namely penetration resistance and oxygen concentration. The complexity of soil structure also causes large spatial variation in soil chemical and biological properties (Wang et al., 2020) and it is likely that root responses to these heterogeneities also differ between species and genotypes. Thus, differentiating between reversible and irreversible root phenotypic plasticity will be crucial to understand how plants explore structurally heterogeneous soil and how this affects resource acquisition and whole plant growth.

Funding

The Swedish Governmental Agency for Innovation Systems (Vinnova; grant number: 2018-02346).

Author contribution

TC, AGB and TK conceived the study; Experimental set-ups were developed by DI, NK, and TC; HS performed experiments and analysed the data together with TC; The manuscript was written by HS and TC with input from all co-authors. Funding was acquired by TC and TK.

Declaration of Competing Interest

The authors declare that they have no known competing financial interests or personal relationships that could have appeared to influence the work reported in this paper.

Acknowledgements

Tino Colombi was funded through a postdoctoral fellowship by the Swedish Governmental Agency for Innovation Systems (Vinnova; grant number: 2018-02346), which is greatly acknowledged. The authors thank Ana María Mingot Soriano (Department of Soil and Environment, SLU, Uppsala) for the analysis of soil physical properties.

Appendix A. Supplementary data

Supplementary material related to this article can be found, in the online version, at doi:https://doi.org/10.1016/j.envexpbot.2021.104494.

References

Angers, D.A., Caron, J., 1998. Plant-induced changes in soil structure: processes and feedbacks. Biogeochemistry 42, 55–72. https://doi.org/10.1023/A:1005944025343.

Araki, H., Iijima, M., 2001. Deep rooting in winter wheat: rooting nodes of deep roots in two cultivars with deep and shallow root systems. Plant Prod. Sci. 4, 215–219. https://doi.org/10.1626/pps.4.215.

Araki, H., Hossain, M.A., Takahashi, T., 2012. Waterlogging and hypoxia have permanent effects on wheat root growth and respiration. J. Agron. Crop Sci. 198, 264–275. https://doi.org/10.1111/j.1439-037X.2012.00510.x.

Athmann, M., Kautz, T., Pude, R., Köpke, U., 2013. Root growth in biopores—evaluation with in situ endoscopy. Plant Soil 371, 179–190. https://doi.org/10.1007/s11104-013-1673-5.

Atkinson, J.A., Hawkesford, M.J., Whalley, W.R., Zhou, H., Mooney, S.J., 2020. Soil strength influences wheat root interactions with soil macropores. Plant Cell Environ. 43, 235–245. https://doi.org/10.1111/pce.13659.

Atwell, B.J., 1990a. The effect of soil compaction on wheat during early tillering. III. Fate of carbon transported to the roots. New Phytol. 115, 43–49. https://doi.org/10.1111/j.1469-8137.1990.tb00920.x.

Atwell, B.J., 1990b. The effect of soil compaction on wheat during early tillering. I. Growth, development and root structure. New Phytol. 115, 43–49. https://doi.org/10.1111/j.1469-8137.1990.tb00920.x.

Bailey-Serres, J., Lee, S.C., Brinton, E., 2012. Waterproofing crops: effective flooding survival strategies. Plant Physiol. 160, 1698–1709. https://doi.org/10.1104/pp.112.208173.

Barley, K.P., 1962. The effects of mechanical stress on the growth of roots. J. Exp. Bot. 13, 95–110. https://doi.org/10.1093/jxb/13.1.95.

Belford, R.K., Klepper, B., Rickman, R.W., 1987. Studies of intact shoot-root systems of field-grown winter wheat. II. Root and shoot developmental patterns as related to nitrogen fertilizer 1. Agron. J. 79, 310–319. https://doi.org/10.2134/agronj1987.00021962007900020027x.

Bengough, A.G., Mackenzie, C.J., 1994. Simultaneous measurement of root force and elongation for seedling pea roots. J. Exp. Bot. 45, 95–102. https://doi.org/10.1093/jxb/45.1.95.

Bengough, A.G., McKenzie, B.M., Hallett, P.D., Valentine, T.A., 2011. Root elongation, water stress, and mechanical impedance: a review of limiting stresses and beneficial root tip traits. J. Exp. Bot. 62, 59–68. https://doi.org/10.1093/jxb/erq350.

Bingham, I.J., Bengough, A.G., 2003. Morphological plasticity of wheat and barley roots in response to spatial variation in soil strength. Plant Soil 250, 273–282.

Broughton, S., Zhou, G., Teakle, N.L., Matsuda, R., Zhou, M., O'Leary, Ra., Colmer, T.D., Li, C., 2015. Waterlogging tolerance is associated with root porosity in barley (Hordeum vulgare L.). Mol. Breed. 35, 27. https://doi.org/10.1007/s11032-015-0243-3.

Chimungu, J.G., Loades, K.W., Lynch, J.P., 2015. Root anatomical phenes predict root penetration ability and biomechanical properties in maize (Zea Mays). J. Exp. Bot. 66, 3151–3162. https://doi.org/10.1093/jxb/erv121.

Colombi, T., Braun, S., Keller, T., Walter, A., 2017a. Artificial macropores attract crop roots and enhance plant productivity on compacted soils. Sci. Total Environ. 574, 1283–1293. https://doi.org/10.1016/j.scitotenv.2016.07.194.

Colombi, T., Kirchgessner, N., Walter, A., Keller, T., 2017b. Root tip shape governs root elongation rate under increased soil strength. Plant Physiol. 174, 2289–2301. https://doi.org/10.1104/pp.17.00357.

Colombi, T., Herrmann, A.M., Vallenback, P., Keller, T., 2019. Cortical cell diameter is key to energy costs of root growth in wheat. Plant Physiol. 180, 2049–2060. https://doi.org/10.1104/pp.19.00262.

Correa, J., Postma, J.A., Watt, M., Wojciechowski, T., 2019. Soil compaction and the architectural plasticity of root systems. J. Exp. Bot. 70, 6019–6034. https://doi.org/10.1093/jxb/erz383.

Croser, C., Bengough, A.G., Pritchard, J., 1999. The effect of mechanical impedance on root growth in pea (Pisum sativum). I. Rates of cell flux, mitosis, and strain during recovery. Physiol. Plant. 107, 277–286. https://doi.org/10.1034/j.1399-3054.1999.100304.x.

Croser, C., Bengough, A.G., Pritchard, J., 2000. The effect of mechanical impedance on root growth in pea (Pisum sativum). II. Cell expansion and wall rheology during recovery. Physiol. Plant. 109, 150–159. https://doi.org/10.1034/j.1399-3054.2000.100207.x.

de Mendiburu, F., 2017. Agricolae: Statistical Procedures for Agricultural Research.

Dexter, A.R., 1988. Advances in characterization of soil structure. Soil Tillage Res. 11, 199–238. https://doi.org/10.1016/0167-1987(88)90002-5.

Eissenstat, D.M., 1992. Costs and benefits of constructing roots of small diameter. J. Plant Nutr. 15, 763–782. https://doi.org/10.1080/01904169209364361.

Feng, X., Xiong, J., Hu, Y., Pan, L., Liao, Z., Zhang, X., Guo, W., Wu, F., Xu, J., Hu, E., Lan, H., Lu, Y., 2020. Lateral mechanical impedance rather than frontal promotes cortical expansion of roots. Plant Signal. Behav. 15 https://doi.org/10.1080/15592324.2020.1757918.

Fukao, T., Bailey-Serres, J., 2004. Plant responses to hypoxia - Is survival a balancing act? Trends Plant Sci. 9, 449–456. https://doi.org/10.1016/j.tplants.2004.07.005.

Gill, W.R., Miller, R.D., 1956. A method for study of the influence of mechanical impedance and aeration on the growth of seedling roots. Soil Sci. Soc. Am. J. 20, 154–157. https://doi.org/10.2136/sssaj1956.03615995002000020004x.

Goss, M.J., 1977. Effects of mechanical impedance on root growth in barley (Hordeum vulgare L.). J. Exp. Bot. 28, 96–111. https://doi.org/10.1093/jxb/28.1.96.

Graves, A.R., Morris, J., Deeks, L.K., Rickson, R.J., Kibblewhite, M.G., Harris, J.A., Farewell, T.S., Truckle, I., 2015. The total costs of soil degradation in England and Wales. Ecol. Econ. 119, 399–413. https://doi.org/10.1016/j.ecolecon.2015.07.026.

Iijima, M., Kato, J., 2007. Combined soil physical stress of soil drying, Anaerobiosis and mechanical impedance to seedling root growth of four crop species. Plant Prod. Sci. 10, 451–459. https://doi.org/10.1626/pps.10.451.

IPCC, 2014. Climate change 2014: synthesis report. Contribution of Working Groups I, II and III to the Fifth Assessment Report of the Intergovernmental Panel on Climate Change. https://doi.org/10.1017/CBO9781107415324. Geneva.

Jin, K., Shen, J., Ashton, R.W., Dodd, I.C., Parry, M.A.J., Whalley, W.R., 2013. How do roots elongate in a structured soil? J. Exp. Bot. 64, 4761–4777. https://doi.org/10.1093/jxb/ert286.

Keller, T., Sandin, M., Colombi, T., Horn, R., Or, D., 2019. Historical increase in agricultural machinery weights enhanced soil stress levels and adversely affected soil functioning. Soil Tillage Res. 194, 104293 https://doi.org/10.1016/j.still.2019.104293.

Kirby, J.M., Bengough, A.G., 2002. Influence of soil strength on root growth: experiments and analysis using a critical-state model. Eur. J. Soil Sci. 53, 119–127. https://doi.org/10.1046/j.1365-2389.2002.00429.x.

Kolb, E., Hartmann, C., Genet, P., 2012. Radial force development during root growth measured by photoelasticity. Plant Soil 360, 19–35. https://doi.org/10.1007/s11104-012-1316-2.

Lipiec, J., Horn, R., Pietrusiewicz, J., Siczek, A., 2012. Effects of soil compaction on root elongation and anatomy of different cereal plant species. Soil Tillage Res. 121, 74–81. https://doi.org/10.1016/j.still.2012.01.013.

Lobet, G., Paez-Garcia, A., Schneider, H., Junker, A., Atkinson, J.A., Tracy, S., 2018. Demystifying roots: a need for clarification and extended concepts in root phenotyping. Plant Sci. https://doi.org/10.1016/j.plantsci.2018.09.015.

Lynch, J.P., 2013. Steep, cheap and deep: an ideotype to optimize water and N acquisition by maize root systems. Ann. Bot. 112, 347–357. https://doi.org/10.1093/aob/mcs293.

Lynch, J.P., Wojciechowski, T., 2015. Opportunities and challenges in the subsoil: pathways to deeper rooted crops. J. Exp. Bot. 66, 2199–2210. https://doi.org/10.1093/jxb/eru508.

Malik, A.I., Colmer, T.D., Lambers, H., Setter, T.L., Schortemeyer, M., 2002. Short-term waterlogging has long-term effects on the growth and physiology of wheat. New Phytol. 153, 225–236. https://doi.org/10.1046/j.0028-646X.2001.00318.x.

Malik, A.I., Ailewe, T.I., Erskine, W., 2015. Tolerance of three grain legume species to transient waterlogging. AoB Plants 7, 1–11. https://doi.org/10.1093/aobpla/plv040.

Materechera, S.A., Alston, A.M., Kirby, J.M., Dexter, A.R., 1992. Influence of root diameter on the penetration of seminal roots into a compacted subsoil. Plant Soil 144, 297–303. https://doi.org/10.1007/BF00012888.

Nosalewicz, A., Lipiec, J., 2014. The effect of compacted soil layers on vertical root distribution and water uptake by wheat. Plant Soil 375, 229–240. https://doi.org/10.1007/s11104-013-1961-0.

O'Brien, J., 2019. Exiftoolr: ExifTool Functionality From R.

Pedersen, O., Sauter, M., Colmer, T.D., Nakazono, M., 2020. Regulation of root adaptive anatomical and morphological traits during low soil oxygen. New Phytol. https://doi.org/10.1111/nph.16375.

Pfeifer, J., Faget, M., Walter, A., Blossfeld, S., Fiorani, F., Schurr, U., Nagel, Ka., 2014. Spring barley shows dynamic compensatory root and shoot growth responses when exposed to localised soil compaction and fertilisation. Funct. Plant Biol. 41, 581–597. https://doi.org/10.1071/FP13224.

Pinheiro, J., Bates, D., DebRoy, S., Sarkar, J., 2013. nlme: Linear and Nonlinear Mixed Effects Models.

R Core Team, 2017. R: A Language and Environment for Statistical Computing.

Rabot, E., Wiesmeier, M., Schlüter, S., Vogel, H.J., 2018. Soil structure as an indicator of soil functions: a review. Geoderma 314, 122–137. https://doi.org/10.1016/j.geoderma.2017.11.009.

Rich, S.M., Watt, M., 2013. Soil conditions and cereal root system architecture: review and considerations for linking Darwin and Weaver. J. Exp. Bot. 64, 1193–1208. https://doi.org/10.1093/jxb/ert043.

Saglio, P.H., Rancillac, M., Bruzan, F.F., Pradet, A., Saglio, P.H., Rancillac, M., Bruzan, F. F., Pradet, A., 1984. Critical oxygen pressure for growth and respiration of excised and intact roots. Plant Physiol. 76, 151–154.

Schjønning, P., Akker, J., Keller, T., Greve, M., Lamandé, M., Simojoki, A., Stettler, M., Arvidsson, J., Breuning-Madsen, H., 2015. Driver-pressure-State-Impact-Response (DPSIR) analysis and risk assessment for soil compaction - a european perspective. Adv. Agron. 133, 183–237.

Schlüter, S., Eickhorst, T., Mueller, C.W., 2019. Correlative imaging reveals holistic view of soil microenvironments. Environ. Sci. Technol. 53, 829–837. https://doi.org/10.1021/acs.est.8b05245.

Schneider, H.M., Lynch, J.P., 2020. Should root plasticity Be a crop breeding target? Front. Plant Sci. 11, 1–16. https://doi.org/10.3389/fpls.2020.00546.

Shierlaw, J., Alston, A.M., 1984. Effect of soil compaction on root growth and uptake of phosphorus. Plant Soil 77, 15–28. https://doi.org/10.1007/BF02182808.

Striker, G.G., Insausti, P., Grimoldi, A.A., Vega, A.S., 2007. Trade-off between root porosity and mechanical strength in species with different types of aerenchyma. Plant Cell Environ. 30, 580–589. https://doi.org/10.1111/j.1365-3040.2007.01639.x.

Thomson, C.J., Colmer, T.D., Watkin, E.L.J., Greenway, H., 1992. Tolerance of wheat (Triticum aestivum cvs. Gamenya and Kite) and triticale (Triticosecale cv. Muir) to waterlogging. New Phytol. 120, 335–344.

Tracy, S.R., Black, C.R., Roberts, J.A., Mooney, S.J., 2013. Exploring the interacting effect of soil texture and bulk density on root system development in tomato (Solanum lycopersicum L.). Environ. Exp. Bot. 91, 38–47. https://doi.org/10.1016/j.envexpbot.2013.03.003.

Vaz, C.M.P.P., Manieri, J.M., de Maria, I.C., Tuller, M., 2011. Modeling and correction of soil penetration resistance for varying soil water content. Geoderma 166, 92–101. https://doi.org/10.1016/j.geoderma.2011.07.016.

Walter, A., Silk, W.K., Schurr, U., 2009. Environmental effects on spatial and temporal patterns of leaf and root growth. Annu. Rev. Plant Biol. 60, 279–304. https://doi.org/10.1146/annurev.arplant.59.032607.092819.

Wang, X., Whalley, W.R., Miller, A.J., White, P.J., Zhang, F., Shen, J., 2020. Sustainable cropping requires adaptation to a heterogeneous rhizosphere. Trends Plant Sci. 25, 1194–1202. https://doi.org/10.1016/j.tplants.2020.07.006.

Watkin, E.L.J., Thomson, C.J., Greenway, H., 1998. Root development and aerenchyma formation in two wheat cultivars and one Triticale cultivar grown in stagnant Agar and aerated nutrient solution. Ann. Bot. 81, 349–354.

Weisskopf, P., Reiser, R., Rek, J., Oberholzer, H.R., 2010. Effect of different compaction impacts and varying subsequent management practices on soil structure, air regime and microbiological parameters. Soil Tillage Res. 111, 65–74. https://doi.org/10.1016/j.still.2010.08.007.

White, R.G., Kirkegaard, J.A., 2010. The distribution and abundance of wheat roots in a dense, structured subsoil: implications for water uptake. Plant Cell Environ. 33, 133–148. https://doi.org/10.1111/j.1365-3040.2009.02059.x.

Whitmore, A.P., Whalley, W.R., 2009. Physical effects of soil drying on roots and crop growth. J. Exp. Bot. 60, 2845–2857. https://doi.org/10.1093/jxb/erp200.

Yamauchi, T., Nakazono, M., Inukai, Y., Tsutsumi, N., 2020. Distance-to-Time conversion using gompertz model reveals age-dependent aerenchyma formation in rice roots. Plant Physiol. https://doi.org/10.1104/pp.20.00321 pp.00321.2020.

Ye, H., Song, L., Chen, H., Valliyodan, B., Cheng, P., Ali, L., Vuong, T., Wu, C., Orlowski, J., Buckley, B., Chen, P., Shannon, J.G., Nguyen, H.T., 2018. A major natural genetic variation associated with root system architecture and plasticity improves waterlogging tolerance and yield in soybean. Plant Cell Environ. 41, 2169–2182. https://doi.org/10.1111/pce.13190.

Young, I.M., Montagu, K., Conroy, J., Bengough, A.G., 1997. Mechanical impedance of root growth directly reduces leaf elongation rates of cereals. New Phytol. 135, 613–619. https://doi.org/10.1046/j.1469-8137.1997.00693.x.